

1993

## The Effect of PEO Ratio on Degradation, Calcification and Bone Bonding of PEO/PBT Copolymer (Polyactive)

C. A. van Blitterswijk  
*Leiden University*

J. v.d. Brink  
*Leiden University*

H. Leenders  
*Leiden University*

D. Baaker  
*Leiden University*

Follow this and additional works at: <https://digitalcommons.usu.edu/cellsandmaterials>



Part of the [Biomedical Engineering and Bioengineering Commons](#)

---

### Recommended Citation

van Blitterswijk, C. A.; Brink, J. v.d.; Leenders, H.; and Baaker, D. (1993) "The Effect of PEO Ratio on Degradation, Calcification and Bone Bonding of PEO/PBT Copolymer (Polyactive)," *Cells and Materials*: Vol. 3 : No. 1 , Article 2.

Available at: <https://digitalcommons.usu.edu/cellsandmaterials/vol3/iss1/2>

This Article is brought to you for free and open access by the Western Dairy Center at DigitalCommons@USU. It has been accepted for inclusion in Cells and Materials by an authorized administrator of DigitalCommons@USU. For more information, please contact [digitalcommons@usu.edu](mailto:digitalcommons@usu.edu).



## THE EFFECT OF PEO RATIO ON DEGRADATION, CALCIFICATION AND BONE BONDING OF PEO/PBT COPOLYMER (POLYACTIVE)

C.A. van Blitterswijk\*, J. v.d. Brink, H. Leenders, D. Bakker<sup>1</sup>

Laboratory for Otobiology and Biocompatibility,  
Biomaterials Research Group, University Hospital Leiden, The Netherlands,  
<sup>1</sup>HC Implants B.V., Zernikedreef 6, 2333 CK Leiden, The Netherlands

(Received for publication December 22, 1992, and in revised form March 31, 1993)

### Abstract

In this study, we evaluated the effect of PEO/PBT proportion on the behavior of a range of PEO/PBT segmented copolymers (Polyactive) during subcutaneous and intrabony implantation in the rat. It was demonstrated that varying the PEO proportion affected degradation, calcification and bone-bonding. The PEO/PBT 70/30 and 60/40 showed extensive degradation after 1 year, PEO/PBT 55/45 an intermediate degradation, and the 40/60 and 30/70 copolymers showed little and hardly any degradation respectively. PEO content also affected the degree of calcification. PEO/PBT 70/30 showed extensive and early calcification whereas almost no calcification was seen with PEO/PBT 30/70. Since calcified sites at the periphery of the polymeric implants were locations of preference for bone-bonding to occur, PEO/PBT proportion also influenced bone/PEO/PBT interactions. The materials with the highest PEO content most frequently showed morphological indications of bone-bonding, while the material with 30% PEO showed no bone/biomaterial contact. The differences in bone-bonding activity were also reflected by the occurrence of an electron dense zone at the bone-biomaterial interface which was morphologically similar to that observed for calcium phosphate ceramics.

**Key Words:** Bioactive, bone, bone-bonding, calcium phosphate ceramics, degradation, interface, polyactive, subcutis, calcification.

### \*Address of Correspondence:

C.A. van Blitterswijk  
Laboratory for Otobiology and Biocompatibility,  
University Hospital, Building 54,  
Rijnsburgerweg 10,  
2333 AA Leiden,  
The Netherlands.

Telephone number 31-(0)71-262466

### Introduction

For alloplastic materials, bone-bonding is a property that has been mainly attributed to certain calcium phosphate ceramics [6, 19, 21, 24] and so called glass ceramics and Bioglass [20, 22]. Furthermore, specific surface reactions on titanium might also place this material into the category of bone-bonding biomaterials [16]. Each of these materials has a high elastic modulus and the glasses and ceramics generally have a low fracture toughness. Evidently, the scope of clinical application of bone-bonding biomaterials would be widened by the availability of materials with a lower elastic modulus, for instance elastomeric polymers.

Until recently no bone-bonding polymers were available and most efforts directed towards obtaining materials with a lower elastic modulus than glasses and ceramics has led research groups to pursue the manufacturing of bone-bonding composites. In these composites, the bone-bonding glasses or ceramics are added as a filler [10] or a coating to a polymeric or metallic substrate [15, 31, 34] and this approach seems to be successful. However, the scope of bone-bonding biomaterials would be even further widened by the availability of a polymer which possesses bone-bonding properties without the addition of bone-bonding agents.

Recently Bakker *et al.* [2, 3, 4] described that a specific Poly(ethylene oxide hydantoin) Poly(butylene terephthalate) segmented copolymer (HPEO/PBT 55/45), with a 55/45 distribution in weight between the two segments, possessed properties that fitted in the bonding osteogenesis theory of Osborn and Newesly [25]. When implanted in a porous form near the bony middle ear bulla of the rat, the HPEO/PBT 55/45 copolymer (also known under the trade name Polyactive) showed an intimate contact with bone without an intervening fibrous tissue layer [2]. Furthermore, bone deposition and ingrowth started both from the periphery and center of pores which fitted Osborn's "bioactive" materials in contrast to the so called "biotolerated" materials which are characterized by distance osteogenesis. Another indication of the bone-bonding capacity of the HPEO/PBT 55/45 copolymer was its

similarity at the bone/biomaterial interface as compared to hydroxyapatite ceramics [3]. An electron dense layer was found that showed continuity with the lamina limitans of bone [29] and was similar in morphology to the bonding zone or electron dense layer observed at the hydroxyapatite/bone interface [7, 12, 17, 27]. By several authors, this layer is considered to play an important role in the bone bonding process.

Recent studies have investigated the interactions with bone, of dense HPEO/PBT 55/45 in comparison with PEO/PBT 55/45, lacking the hydantoin segment, together with two calcium phosphate ceramics and silicone rubber [8, 9]. It was reported that both HPEO/PBT 55/45 and PEO/PBT 55/45 bonded with bone as did the calcium phosphate ceramics. During pull out studies, the bonding strength at the bone/biomaterial interface exceeded the internal strength of both polymers and ceramics. This study demonstrated that hydantoin was not necessary for bone-bonding of the copolymer and can therefore be omitted in future studies. In addition, there seemed to be a relationship between the calcification of the polymer's surface and the occurrence of bone-bonding. At such areas, calcium phosphate crystals were seen to penetrate into the polymer, forming a continuity between the crystals in bone and the polymer, partially explaining the bone-bonding mechanism.

Since calcification of the (H)PEO/PBT 55/45 copolymer is possibly related to the PEO segment of the polymer, which as Polyether depending on its molecular weight, would be able to absorb calcium ions [32], we decided to investigate the effects of variation in PEO/PBT proportion. Special emphasis was placed on the assessment of degradation, calcification and bone-bonding, using light microscopy, scanning transmission electron microscopy, X-ray microanalysis and image analysis. The PEO/PBT copolymers, varying in PEO proportion from 30% to 70%, were implanted in the form of dense blocks into the tibia and subcutis of the rat. Calcification was also quantitatively assessed on porous films during subcutaneous implantation in the same animal.

## Materials and Methods

### Implant materials

Five different PEO/PBT block copolymers differing in PEO/PBT proportion (PEO/PBT: 70/30, 60/40, 55/45, 40/60 and 30/70) were used. All polymers were obtained through HC Implants BV (Leiden, The Netherlands). The polymers were in the form of dense smooth blocks (1.5 x 1.5 x 1.5 mm) with the exception of the 55/45 and 30/70 which at the time of the study were only available in a cylindrical form of similar dimensions. Furthermore, all materials were also used as porous films. The molecular weight of the individual PEO segments was 1000 Dalton (D).

### Implantation site and procedure

Both blocks and porous films were implanted

subcutaneously after dorsal incisions. Blocks were also implanted into the rat tibia, no press fit procedure was used and the implants were loosely inserted into the created defect (greater than  $\pm 2$  mm). Male Wistar rats of 180-200 grams body weight were used. As post-operative evaluation intervals, we chose 3 weeks, 6 weeks, 3 months, 6 months and 12 months. For each PEO/PBT proportion and implant type (blocks and films), 4 implants were used per implantation site and interval, thus representing a total of 200 blocks and 100 films distributed over 50 animals.

### Evaluation techniques

As evaluation techniques, we used light microscopy, scanning electron microscopy (Philips 525), transmission electron microscopy (Philips 201, 400, 410), back-scattered electron microscopy, X-ray microanalysis (TN 2000, Voyager) and image analysis (Vidas). Both decalcified and non-decalcified material were studied. All specimens were fixed in glutaraldehyde and those destined for transmission electron microscopy were post-fixed in 1% osmium tetroxide. The films (4 per type and interval) were only analyzed by light microscopy and alizarin red staining (indicative for calcium) while in the case of the blocks, two were used for light microscopy, one for scanning and one for transmission electron microscopy. Back-scattered electron microscopy was mostly performed on either Epon or glycol methacrylate embedded blocks obtained after sectioning and on corresponding sections, all sputter-coated with carbon. A more elaborate description of the techniques has been reported in earlier publications [8].

### Determination of calcification

For each implant type and postoperative interval, 4 films were sectioned in 2  $\mu$ m sections with a LKB Ultracut 2000. Subsequently, 5 sections were analyzed by a Vidas image analysis system for the presence of calcium, based on alizarin red staining. The polymers were visualized by sudan black staining and/or polarized light and the tissue morphology and boundaries were assessed using a toluidine blue stain.

## Results

### Subcutaneous implantation

**General tissue reactions:** All blocks showed similar reactions concerning the surrounding fibrous tissue when studied by light microscopy. Initially (3 weeks) the blocks were partially surrounded by a loosely arranged fibrous tissue, incorporating some inflammatory cells (Fig. 1). After longer implantation times, a thin zone of dense fibrous tissue with collagen fibers running parallel to the surface was observed. Fibroblasts within the capsule assumed a similar orientation. Although large areas near the implant surface lacked the presence of inflammatory cells, both macrophages and multinucleated cells could be observed at some locations. The use of scanning and transmission

electron microscopy confirmed these light microscopical findings. It should be emphasized that the above description of the tissue surrounding the implant largely refers to those implants with their surface predominantly intact. After one year such an intact surface was only observed for the PEO/PBT 30/70 and 40/60 copolymers. All other PEO/PBT proportions showed a clear alteration of the implant structure.

**Implant degradation:** The first indications of a change in implant structure were observed for the PEO/PBT 70/30 copolymer. This polymer already showed degradation into relatively large fragments three weeks following implantation, which was most clearly observed by scanning electron microscopy. Due to the relatively large size of the individual fragments most of the implant/tissue interface of this copolymer was still composed of a morphologically intact polymer surface. At 6 weeks the degradation of PEO/PBT 70/30 had progressed and PEO/PBT 60/40 showed the first signs of fragments detaching from its surface. All other PEO/PBT proportions were still generally intact, except for crack formation at their surface in a confined zone of approximately 10-100  $\mu\text{m}$  thickness. After 3 months, both the 70/30 and 60/40 proportion showed extensive fragmentation throughout and fibrous tissue had filled the interfragment space. At this point in time, the PEO/PBT 55/45 also showed extensive crack formation and detachment of fragments from the implant surface although the implant outline was still largely intact. Crack formation in the PEO/PBT 40/60 had proceeded but fragment detachment was not yet apparent. The PEO/PBT 30/70 did not reveal significant changes as compared to the 6 weeks period. In the 6 month and 1 year periods, fragmentation had continued for the PEO/PBT 70/30, 60/40 and 55/45 copolymer causing a smaller average particle size in the course of time. For the PEO/PBT 70/30 proportion, fragmentation was so extensive that the implants were difficult to retrieve after 1 year. The PEO/PBT 40/60 and 30/70 did not show a significant deviation from the 3 month period with exception of the occurrence of a single deep crack in one of the 40/60 implants after one year. Figures 2a-d show the situation for the various PEO/PBT proportions after long term implantation. With exception of the 1 year PEO/PBT 70/30, the original contours of the implants could still be observed despite the fact that tissue had grown into the interfragment space. This indicated that the disappearance of implant material from the actual implantation site, was either by cellular transport or actual resorption. Light microscopical surveys of general degradation are shown in Figures 3a-c.

**Cellular reactions during degradation:** The degradation found for the different PEO/PBT proportions had major consequences for the tissue that surrounded the implants and penetrated into the interfragment space. Light microscopy revealed that, in the early stages of fragment detachment, phagocytes were present near the implant surface with implant particles

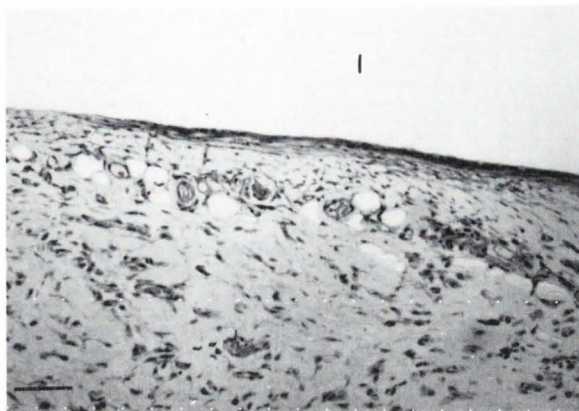


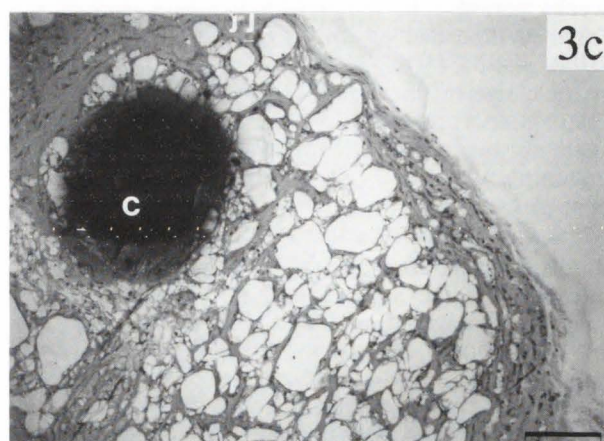
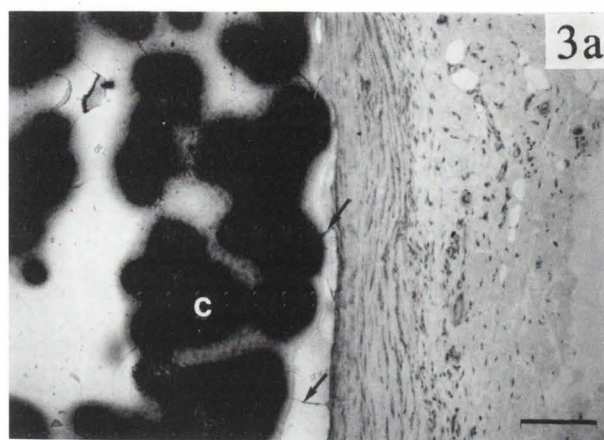
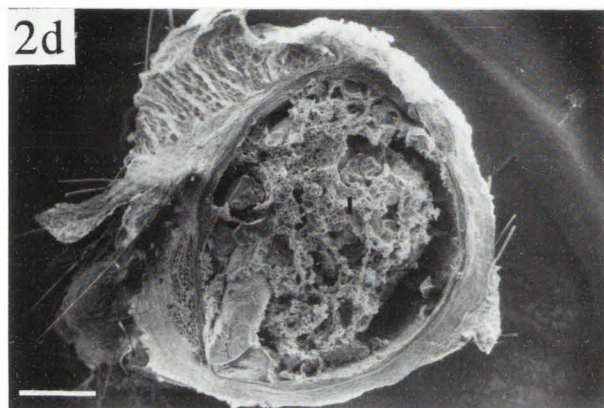
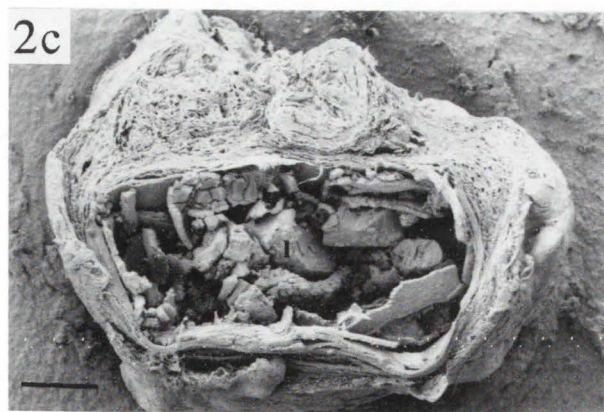
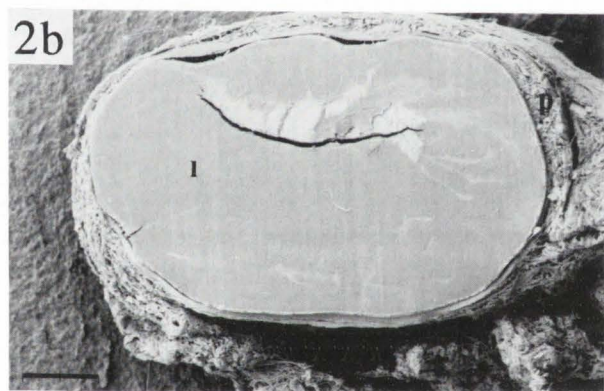
**Figure 1.** Light micrograph of a dense 70/30 PEO/PBT implant (I) after 6 weeks of subcutaneous implantation. Bar = 150  $\mu\text{m}$ .

in their cytoplasm. As fragmentation continued, these cells were also seen in the interfragment spaces. The more extensive fragmentation became, the more prominent these cells were and the higher their extent of cytoplasmic loading. Eventually, the phagocytes in the heavily degrading PEO/PBT proportions assumed a foam cell appearance. Transmission electron microscopy showed the extent of phagocytosis of implant material even more clearly (Fig. 4). In spite of the heavy loading of these cells with implant fragments, their general morphology remained relatively normal (Fig. 5). The nucleus was always intact and all cell organelles were present. The high amount of, frequently dilated, rough endoplasmic reticulum and mitochondria suggested a high metabolic activity. The orientation and morphology of fragments in the cell cytoplasm sometimes suggested that fragmentation would even continue within the cytoplasm.

#### Subcutaneous calcification

**General observations:** When investigating the polymers, it was observed that zones were present in the polymer that stained positive during alizarin red staining, indicating the presence of calcium. The presence of both calcified spots and larger calcified areas with quite frequently spots at their internal periphery (Fig. 6) suggested that calcification started by focal points gradually leading to larger calcified areas. Calcified areas were also clearly visible using scanning electron microscopy combined with single spot analysis or with backscatter electron microscopy (Figures 7a-d; at color plate page 33). The composition of these calcified areas will be further elucidated below when discussing the interactions of the PEO/PBT copolymers with bone. Calcification was more prominent with increasing PEO content and no calcification was observed with the 30/70 copolymer.

**Quantification of calcification:** Since quantitative evaluation of the calcification in the blocks was



difficult to perform, we decided to use the porous polymer films for quantitation. In general, the films showed an apparently faster degradation than the blocks. Due to this rapid degradation, it was no longer possible to retrieve the 70/30 films after periods longer than 3 months. The polymers were well recognized by sudan black staining and calcification was assessed by alizarin red staining (Fig. 8). The results, obtained after image analysis, are shown in Fig. 9

**Figure 2 (facing page, left).** Scanning electron micrographs of different dense PEO/PBT implants after subcutaneous implantation. Sometimes the porous film is also visible. I = dense implant, p = porous film. a) PEO/PBT 30/70, 1 year after implantation showing no noteworthy signs of degradation. Bar = 0.63 mm. b) PEO/PBT 40/60, only shows confined crack formation after 1 year of implantation. Bar = 0.56 mm. c) PEO/PBT 60/40 with prominent fragmentation, 1 year after implantation. Bar = 0.67 mm. d) PEO/PBT 70/30, characteristically showed extensive fragmentation and disappearance of bulk material, 6 months after implantation. Bar = 0.69 mm.

**Figure 3 (facing page right).** Light micrographs of increasing stages of fragmentation during subcutaneous implantation. C = calcified area (alizarin red staining). a) PEO/PBT 55/45 after 1 year of implantation. The first signs of fragmentation are seen in the form of crack formation of the interface (arrows). Bar = 300  $\mu\text{m}$ . b) PEO/PBT 60/40 implanted for 1 year showing the second stage of fragmentation, more extensive surface erosion leading to detachment of implant fragments (arrows). Bar = 300  $\mu\text{m}$ . c) PEO/PBT 70/30 after 1 year of implantation showing extensive fragmentation throughout the polymer. Bar = 300  $\mu\text{m}$ .

**Figure 4 (at right, top).** Phagocytes near the implant surface. (I) heavily loaded with polymer fragments (arrows). Transmission electron micrograph. Bar = 3.1  $\mu\text{m}$ .

**Figure 5 (at right, middle).** A more detailed micrograph of the cytoplasm of a cell that phagocytosed PEO/PBT 70/30 (arrows) 6 months after subcutaneous implantation. Note the normal morphology of the cell organelles. Bar = 0.94  $\mu\text{m}$ .

which indicates that more PEO will lead to increased calcification. This seems to suggest that an increase in PEO content will also lead to earlier calcification. In correspondence with the blocks, no calcification was found for the 30/70 copolymer. It was interesting to note that with the exception of the PEO/PBT 40/60 copolymer, none of the implanted films showed significant calcification at the 3 month period. In contrast, calcification could still be found with the blocks at this stage.

#### Implantation into the tibia

The degradation behavior of the PEO/PBT copolymers has already been discussed in the **Subcutaneous implantation** section above. The mechanism of degradation in bone did not significantly deviate from that in the subcutaneous implantation site, although it generally seemed less prominent, therefore degradation will not be further discussed in this section and the results will be confined to bone/biomaterial interactions.

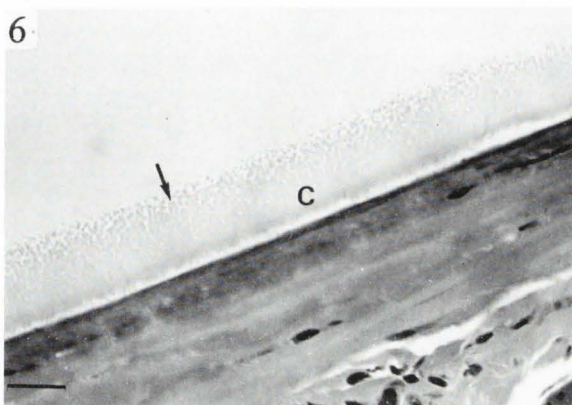
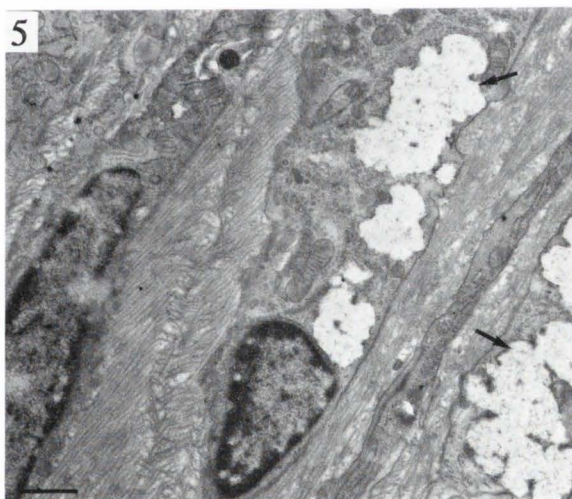
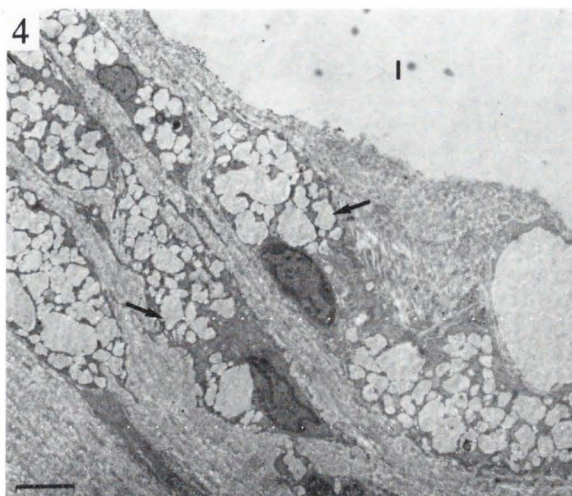


**Figure 6.** The interfacial zone of a PEO/PBT 55/45 with fibrous tissue after 1 year of implantation. Extensive calcification (C) is found near the implant surface with spot-like calcification seen at greater distances (arrow). Bar = 60  $\mu\text{m}$ .

Table 1. Degradation of PEO/PBT copolymers after 3 and 6 weeks (w), and 3, 6, and 12 months (m).

PEO/PBT	3w	6w	3m	6m	12m
70/30	+++	+++	++++	++++	+++++
60/40	+	++	+++	++++	++++
55/45	-	+	++	+++	+++
40/60	-	-	+	+	+ / ++
30/70	-	-	-	-	-

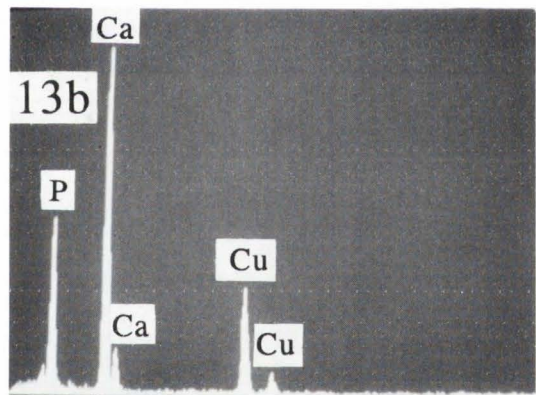
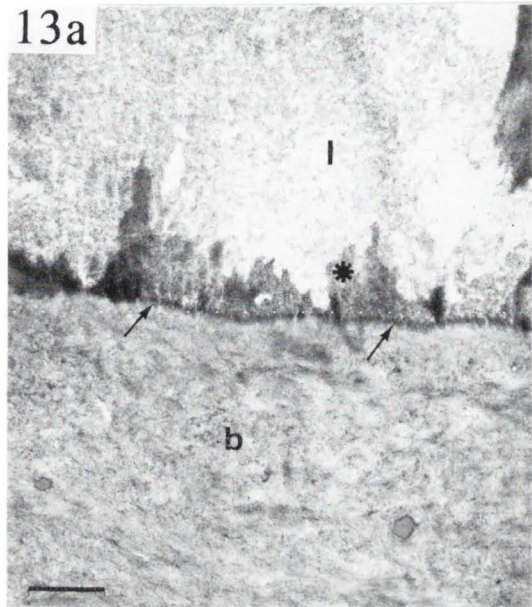
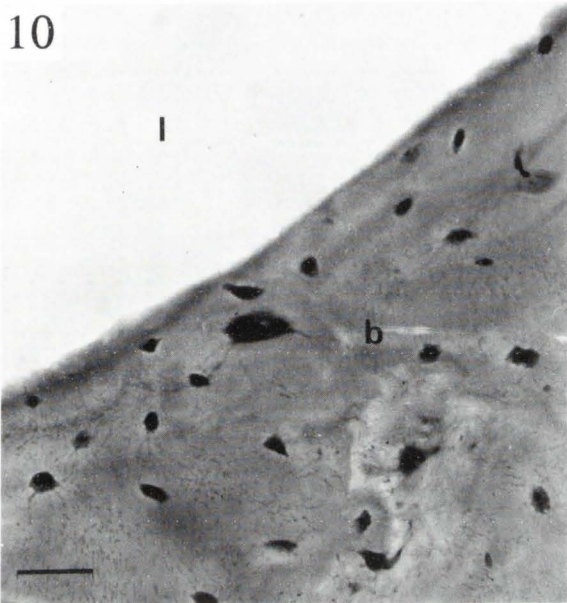
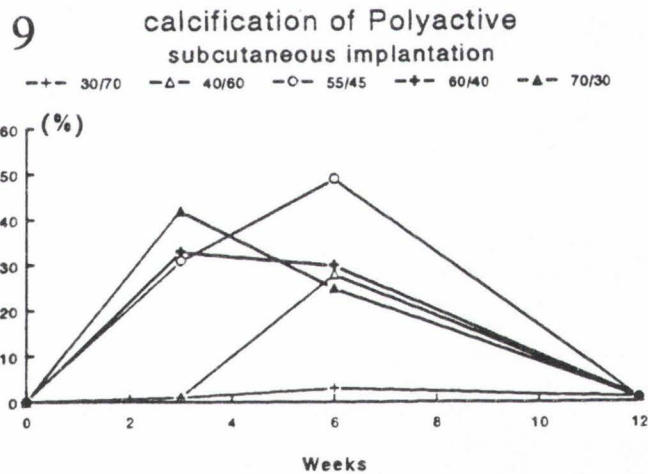
- Superficial crack formation
- + Crack formation within bulk of material
- ++ Fragments detaching from surface
- +++ Fragmentation into large particles
- ++++ Degradation into smaller particles
- +++++ Extensive degradation

Light microscopical evaluation of the various PEO/PBT implants showed rather similar reactions. All implants were covered by fibrous tissue, bone marrow, and bone. The bone was of a lamellar type and after longer implantation times, large parts of the polymer were covered by this type of tissue (Fig. 10).

**Evaluation of non-decalcified material:** Analysis of the bone/biomaterial interface by scanning and transmission electron microscopy and backscatter electron microscopy in combination with X-ray microanalysis showed that, with exception of the PEO/PBT 30/70 copolymer, all copolymers had areas of intimate bone contact. With PEO/PBT 30/70 areas of contact were present at the light microscopical level, but this observation was never confirmed by electron microscopy. Electron microscopy always showed areas of non-calcified tissue either composed of cellular or collagenous material. Concerning the other polymers, it should be emphasized that the data were suggestive of an increase in the incidence of intimate contact, in time and in quantity, with increasing PEO content. However, due to the relatively small number of implants investigated, this presumption could not be proven. The general appearance of the bone-polymer interface is illustrated by the use of back-scattered electron microscopy in Figures 11a-c (on color plate, at page 33) which shows a polished, non-decalcified, Spurr embedded PEO/PBT 60/40 implant, 3 months

after implantation. The X-ray maps provided in Fig. 11 demonstrated that the tissue surrounding the implant in the marrow cavity was indeed composed of bone, as indicated by the presence of calcium and phosphorus signals. A higher magnification of the area near the cortex, combined with X-ray map (Figures 12a-c; at color plate on page 33), showed that the bone was in continuity with what seemed to be calcified spots in the implant material. Analysis of these areas by transmission electron microscopy showed calcified areas throughout the polymer and near bone. Higher magnifications demonstrated that such spots were composed of needle-like crystals. The similarity between the crystals in the polymer and those in bone is stressed by Figures 13a and b, which show a calcified area in the polymer surface opposed to bone. Furthermore, an electron dense zone could sometimes be seen at the interface in these locations.

**Analysis of decalcified material:** Study of the decalcified bone/PEO/PBT copolymer interface was predominantly performed with transmission electron microscopy. Although the morphology of the interface showed some variation, an interesting structure was seen at the interface of all materials except for the 30/70 PEO/PBT copolymer. This latter material never showed a clear contact with bone and sometimes a non-calcified lamellar structure was seen interposed between bone and the polymer (Fig. 14a). At the



Figures 7, 11, & 12 are on color plate, page 33.

**Figure 8 (top left).** Light micrograph showing a porous PEO/PBT 60/40 film after 6 weeks of implantation. The major part of the implant fragments are calcified as indicated by the Alizarin red staining (arrows). Bar = 250  $\mu$ m.

**Figure 9 (middle left).** Diagram showing the calcification in different PEO/PBT proportions as a percentage of total PEO/PBT surface.

**Figure 10 (bottom left).** Light micrograph showing a general view of a decalcified PEO/PBT 60/40 interface with bone after 6 months. Bar = 60  $\mu$ m. I = implant, b = bone.

**Figure 13 (above).** a) Transmission electron micrograph of the non-decalcified PEO/PBT 60/40 interface with bone after 3 months. Note the presence of small needle-like crystals in both the bone (b) and the implant (I). Note the electron dense zone at the interface (arrows). Bar = 1.1  $\mu$ m. b) Spot analysis (at \*) shows the presence of Ca and P throughout the polymer. Copper peaks are from the grid.

bone/biomaterial interface of all materials with a PEO content of 40% per weight or more, an electron dense deposit was encountered. In the case of the PEO/PBT 40/60, this zone was composed of focal floccular material but it was unclear whether it was located on the surface or also in the implant material (Fig. 14b). A similar structure was found with the PEO/PBT 55/45 material, however, it was more continuous and frequently had a multilayered structure above (Fig. 14c). The PEO/PBT 60/40 mostly lacked the floccular deposit found with the 55/45 and 40/60 materials, here only a prominent multilayered structure was seen (Fig. 14d). A similar structure was observed with the PEO/PBT 70/30 copolymer (Fig. 14e). With the latter type of material, it was characteristic that part of the multilayered electron dense structure was located in the actual polymer. This latter phenomenon was never clearly demonstrated for the other PEO/PBT proportions.

### Discussion

Varying the PEO/PBT proportion of PEO/PBT copolymer had several effects. First, PEO/PBT proportion directly influenced the degradation rate of the copolymer. The fastest degradation rate was observed for the PEO/PBT 70/30 copolymer, which was almost completely degraded after 1 year, while the PEO/PBT 30/70 showed hardly any degradation at all after this period. The other copolymers showed an intermediate degradation which increased with PEO concentration (Table 1). The mechanism of degradation is still not completely clear but based on our current knowledge it seems to comprise at least two factors. The first involves hydrolysis of the polymer matrix which will attack the ester bonds in the polymer. Varying the PEO/PBT proportion can influence hydrolysis in more than one way. It will change the amount of available ester bonds and by increasing the PEO content of the copolymer it, being a hydrogel, will take up more water thus facilitating the hydrolysis process. The second process involves a surface erosion as reported in this study. Fragmentation initially starts at the material surface, presumably by mechanical factors, and then proceeds to the core of the implant. At the surface of each fragment degradation will continue in a similar way. The consequence of these two factors would be that, if an implantation site influences the polymers accessibility to water or the mechanical friction at its surface (i.e., between material and subcutaneous layer), then this might affect the implants degradation rate. Of course, other mechanisms of degradation, such as enzymatic attack, also need to be investigated.

The degradation and fragmentation of the polymer has consequences for its general biocompatibility. It was striking to observe that fragmentation led to excessive phagocytosis of fragments by cells that eventually assumed the morphology of foam cells. This indicated that cells could still phagocytose despite the

presence of relatively high amounts of material that had already been phagocytosed. In general, cell morphology remained intact and, in spite of the sometimes extensive fragmentation, no local inflammatory response was observed other than the presence of the phagocytosing cells. These data deviated from findings described for polylactide and associated polymers, where an extensive inflammatory reaction was reported during the degradation stage [4, 28]. Since substantial degradation of the PEO/PBT copolymers can occur, it will be necessary to further analyze the degradation route and products. However, the experimental data and those in the literature do not indicate any adverse effects associated with degradation of these copolymers [1, 4, 5, 18, 26, 30, 35].

Varying the PEO/PBT ratio did not only influence degradation rate but also the calcification of the polymer. Calcification of polymers is a well known phenomenon and several studies have been dedicated to preventing this. Part of those studies indicate that PEO or PTMO homopolymers with a molecular weight of 1000 D showed a peak in calcium absorption [32]. The molecular weight of the PEO used in this study was 1000 D and as the calcification rate increased with PEO content, it is likely that calcification of the PEO/PBT copolymer is indeed related to calcium absorption by the PEO fragment. It was interesting to note that the quantitative assessment of calcification in the porous films indicated that it was a reversible process, at least in soft tissue. With the exception of the PEO/PBT 40/60, which apparently shows an overall delayed and less distinct reaction, no significant calcification was found at implantation periods of three months and more. It should be emphasized, however, that the quantitation was only based on porous films after subcutaneous implantation and other implant shapes and/or implantation sites may show different calcification patterns. This was actually confirmed by the fact that extensive calcification could still be found in the dense blocks after longer implantation times irrespective of the fact whether they were implanted subcutaneously or in bone. Although calcium absorption by the PEO segment must play a role in the calcification it is still not clear how the precipitation of calcium phosphate occurs and why it occurs at specific sites, such as just beneath the surface of the implant material. The data presented in the current study suggest that calcification initially occurs by the formation of needle-shaped calcium phosphate crystals, not unlike hydroxyapatite, in mineralization nodules. In later stages, the merging of mineralization nodules might lead to the larger calcified areas which were frequently observed near the surface or in the center of the dense blocks.

Calcification near the surface of the polymers plays an important role in the bone-bonding process. This is stressed by the fact that our current data support the view that PEO/PBT 30/70, which shows no significant calcification, never revealed an intimate

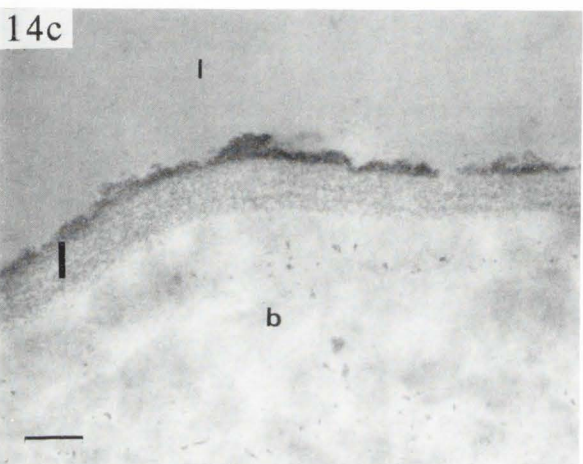
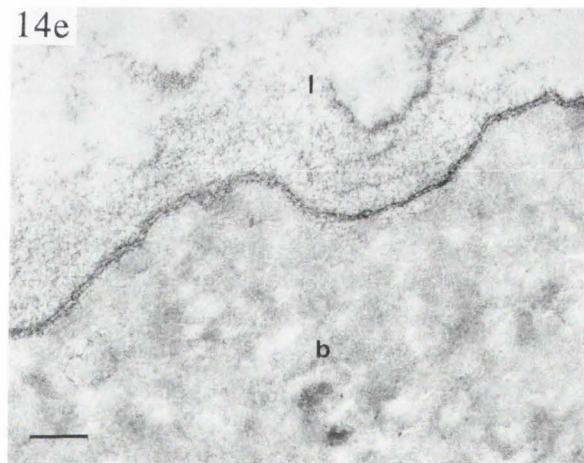
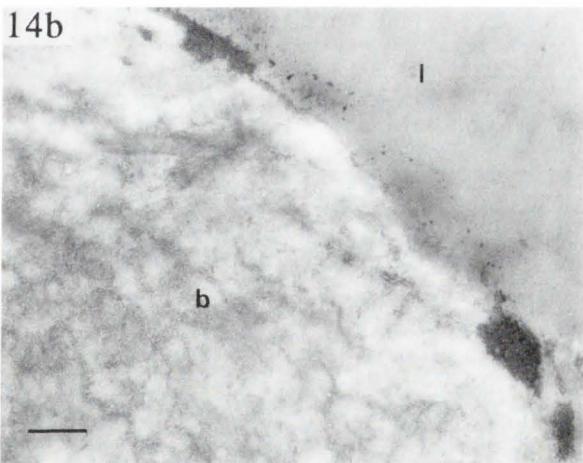
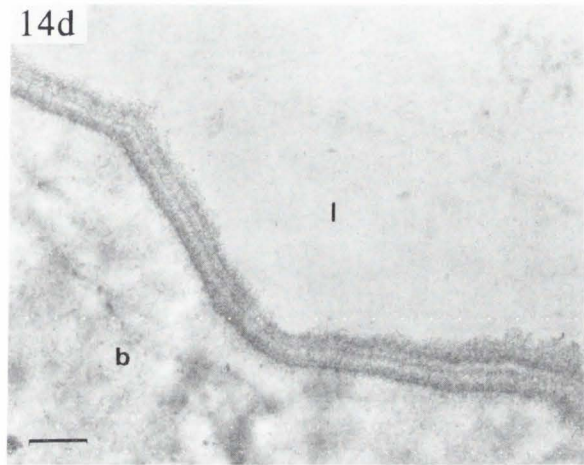
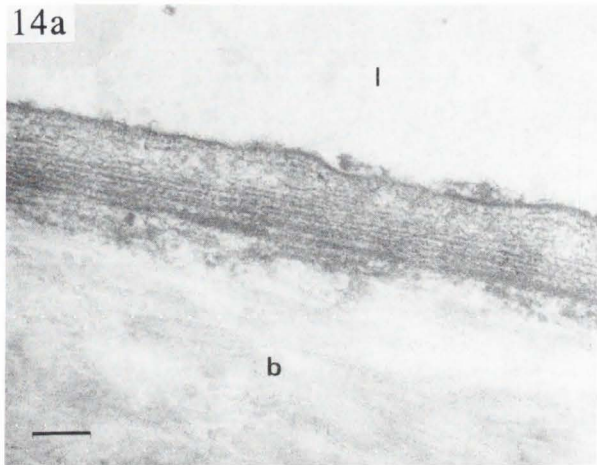


**Figure 14.** The interface between bone and different PEO/PBT proportions. All specimens were decalcified prior to embedding. Note the electron dense structure at the bone/PEO/PBT interface. An interposed fibrillar zone was always found between bone matrix and PEO/PBT 30/70. I = implant, b = bone.

- a) PEO/PBT 30/70, 6 months. Bar = 0.28  $\mu\text{m}$ .
- b) PEO/PBT 40/60, 6 weeks. Bar = 0.37  $\mu\text{m}$ .
- c) PEO/PBT 55/45, 6 weeks. Bar = 0.20  $\mu\text{m}$ .
- d) PEO/PBT 60/40, 6 weeks. Bar = 0.38  $\mu\text{m}$ .
- e) PEO/PBT 70/30, 6 weeks. Bar = 0.41  $\mu\text{m}$ .

contact with bone at its interface. All other PEO/PBT proportions used in this study, that did calcify, did show such an intimate contact with bone. Furthermore, the relationship between bone-bonding and calcification became clear by two other observations. First, the materials that showed most calcification were also characterized by the most bone/biomaterial contact, although it should be emphasized that this was only assessed subjectively and needs quantitative support. Second, many sites of intimate contact with bone were found at sites of copolymer calcification. Possibly a calcified surface is a preferential site of bone contact. Further analysis of the non-decalcified bone/biomaterial interface showed a "continuity" between the hydroxyapatite crystals of bone and the calcium phosphate crystals in the polymer. This continuity might at least partially explain the bonding that occurs at the interface and is not unlike the bonding mechanism described for both "bioactive" glasses and ceramics [7, 11, 20, 23, 25, 33].

This similarity between the more traditional bone-bonding biomaterials and PEO/PBT copolymer was not confined to the non-decalcified interface but extended to the decalcified interface as well. Bakker *et al.* [3] have described that investigation of the (H)PEO/PBT copolymer/bone interface revealed a structure that was similar to the electron dense zone found for hydroxyapatite ceramic at sites of bone contact. The exact composition of this structure is still not completely clear but it is composed of organic matrix (rich in glycosaminoglycans) [12], anorganic material (calcium phosphate crystals) [7], is related to the lamina limitans of bone [27], and shows some similarities with cement lines and/or reversal lines [14]. Several authors assume that there might be a relationship between the occurrence of bone bonding and the presence of this particular structure, therefore, it was interesting to note that the non bone-bonding PEO/PBT 30/70 did not show such a structure. Furthermore, the morphology of the electron dense zone with the other polymers was clearly related to the PEO/PBT proportion. The PEO/PBT 70/30 was characterized by a multilayered structure clearly penetrating the materials surface whereas the PEO/PBT 40/60 only showed an electron dense focal deposit. The PEO/PBT 55/45 showed a combination of the previous two polymers in the shape of both an electron dense deposit, albeit more continuous, and a multilayered structure. This difference in morphology of the electron dense layer at the bone/biomaterial interface seen for PEO/PBT copolymer corresponds with the variations reported for this structure with calcium phosphate ceramics that vary in crystal structure [6, 7, 13].

In conclusion, it can be stated that variation in PEO/PBT proportion will change the degradation rate, calcification and bone bonding capacity of PEO/PBT copolymers. Future studies will be directed towards the quantification of this phenomenon and to investigate whether variations in molecular weight of the

Figures 7, 11, and 12 on color plate, page 33.

**Figure 7.** Ultrastructural analysis of PEO/PBT calcification. **a)** Calcified spots as seen by scanning electron microscopy at the surface of a PEO/PBT 70/30 fragment, 3 months after subcutaneous implantation. Bar = 2  $\mu\text{m}$ . **b)** A cross-section of spot-like calcified areas within PEO/PBT 60/40 after 1 year subcutaneously. Note the needle-like crystallites. Bar = 1.6  $\mu\text{m}$ . **c)** Back-scattered electron micrograph of a calcified spot (\*) within PEO/PBT 55/45 just below the surface after 3 months of subcutaneous implantation. Bar = 31.7  $\mu\text{m}$ . **d)** X-ray map indicating the presence of calcium in the structure shown in Figure 7c.

**Figure 11.** **a)** Back-scattered electron micrograph of an undecalcified PEO/PBT 60/40 after 3 months implantation. I = implant, b = bone. Bar = 0.6  $\mu\text{m}$ . **b and c)** X-ray maps indicating the presence of calcium (b) and phosphorus (c).

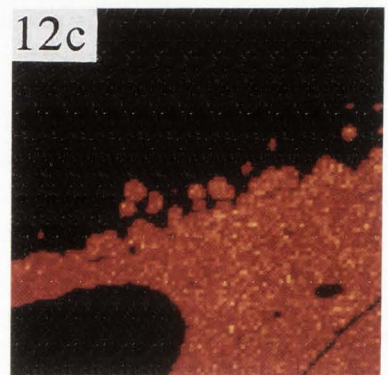
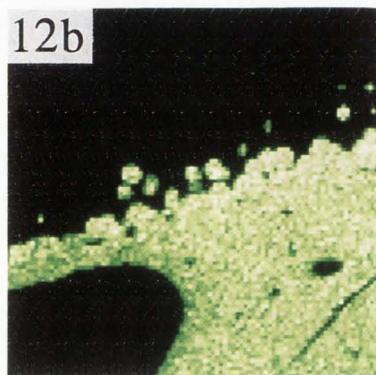
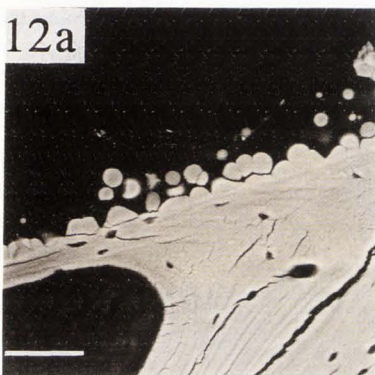
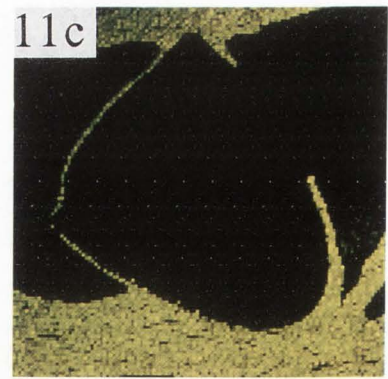
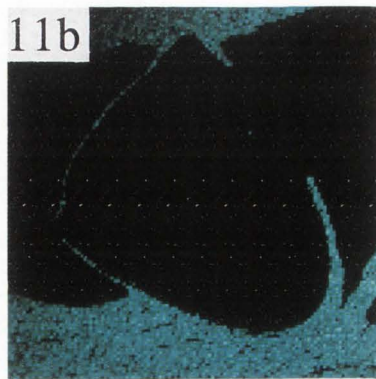
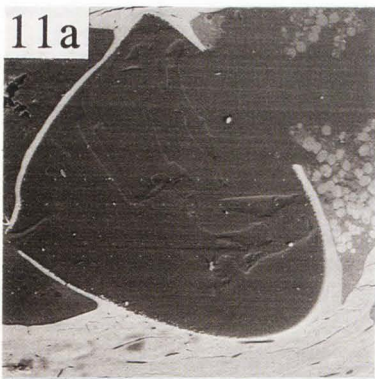
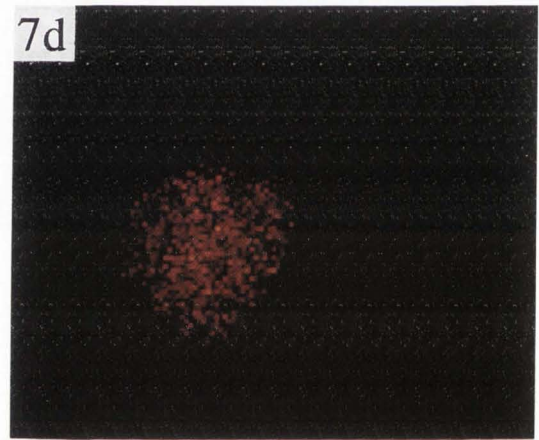
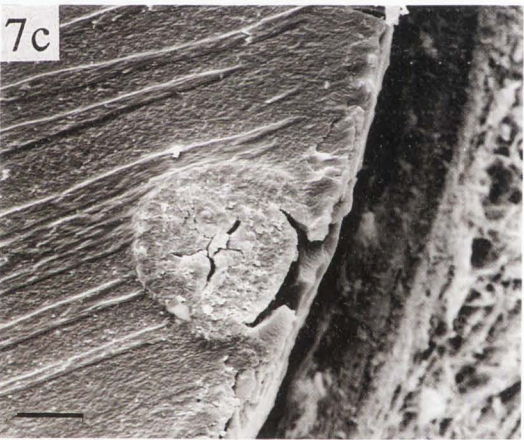
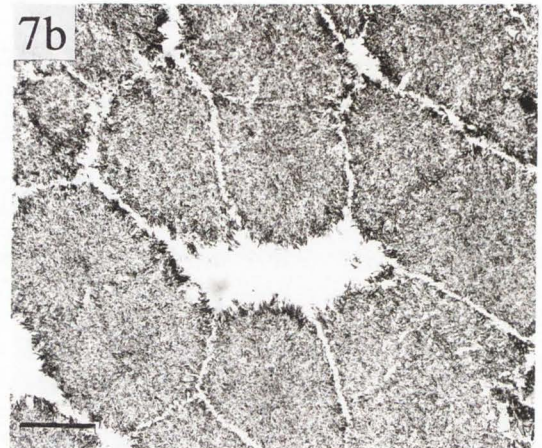
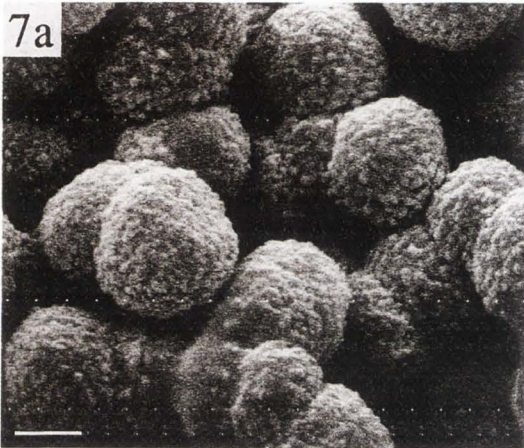
**Figure 12.** More detailed back-scattered electron micrograph. I = implant, b = bone. Bar = 52  $\mu\text{m}$ . **a)** undecalcified PEO/PBT 60/40 after 3 months. **b and c)** X-ray map indicating the presence of calcium (b) and phosphorus (c).

PEO segment will affect the aforementioned properties in a way similar to variations in PEO/PBT proportion.

#### References

1. Autian J (1973). Toxicity and health threats of phthalate esters: Review of the literature. *Env. Health Respect* **4**, 3-26.
2. Bakker D, Blitterswijk CA van, Hesselings SC, Koerten HK, Kuijpers W, Grote JJ (1990). Biocompatibility of a polyether urethane, polypropylene oxide and a polyether polyester copolymer. A qualitative and quantitative study of three alloplastic tympanic membranes materials in the rat middle ear. *J. Biomed. Mater. Res.* **24**, 489-515.
3. Bakker D, Blitterswijk CA van, Hesselings SC, Daems WTh, Grote JJ (1990). Tissue/Biomaterial interface characteristics of four elastomers. A transmission electron microscopical study. *J. Biomed. Mater. Res.* **24**, 277-293.
4. Bakker D, Blitterswijk CA van, Daems WTh, Grote JJ (1988). Biocompatibility of six elastomers in vitro. *J. Biomed. Mater. Res.* **22**, 423-439.
5. Beumer GJ, Bakker D, Blitterswijk CA van, Ponc M (1990). A new cell seeded artificial skin for the treatment of deep dermal wounds. In: *Clinical Implant Materials*. Elsevier, 169-174.
6. Blitterswijk CA van, Grote JJ, Koerten HK, Kuijpers W (1986). The biological performance of calcium phosphate ceramics in an infected implanted site. III. Biological performance of  $\beta$ -whitlockite in the

PEO ratio affects Polyactive/tissue interactions



infected and non-infected rat middle ear. *J. Biomed. Mater. Res.* **20**, 1197-1217.

7. Blitterswijk CA van, Grote JJ, Kuijpers W, Blok-van Hoek CJG, Daems WTh (1985). Bioreactions at the tissue/hydroxyapatite interface. *Biomaterials* **6**, 243-251.

8. Blitterswijk CA van, Wijn JR de, Leenders H, Brink I van den, Hesseling SC, Bakker D (1993). A comparative study of the interactions of two calcium phosphates PEO/PBT copolymer (polyactive) and a silicone rubber with bone and fibrous tissue. *Cells and Materials* **3**, 11-22 (this issue).

9. Blitterswijk CA van, Bakker D, Hesseling SC, Koerten HK (1991). Reactions of cells at implant surfaces. *Biomaterials* **12**, 187-193.

10. Bonfield W, Doyle C, Tanner KF (1986). *In vivo* evaluation of hydroxyapatite reinforced polyethylene composites. In: *Biological and Mechanical Performance of Biomaterials*. Elsevier, 153-158.

11. Bonfield W, Lublinska ZB (1991). High resolution microscopy of a bone implant interface. In: *The Bone Biomaterial Interface*. University of Toronto Press, Canada, 89-94.

12. Bruijn JD de, Klein CPAT, Groot K de, Blitterswijk, CA van (1992). The ultrastructure of the bone-hydroxyapatite interface *in vitro*. *J. Biomed. Mater. Res.* **26**, 1365-1382.

13. Bruijn JD de, Davies JE, Flach JS, Groot K de, Blitterswijk CA van (1991). Ultrastructural of the mineralized tissue/calcium phosphate interface *in vitro*. In: *Tissue Inducing Biomaterials*. Mater. Res. Soc. Symp. Proc. **252**, 63-70.

14. Davies JE, Ottensmeyer P, Shen X, Hashimoto M, Peel SAF (1991). Early extracellular matrix synthesis by bone cells. In: *The Bone Biomaterial Interface*. University of Toronto Press, Canada, 214-218.

15. Dhert WJA, Klein CPAT, Wolke JGC, Velde EA van der, Groot K de, Rozing PM (1991). A mechanical investigation of fluorapatite magnesium whitlockite and hydroxyapatite plasma-sprayed coatings in goats. *J. Biomed. Mater. Res.* **25**, 1183-1200.

16. Ducheyne P, Healy K (1991). Titanium: Inversion induced surface chemistry charges and the relationship to passive dissolution and bioactivity. In: *The Bone Biomaterial Interface*. University of Toronto Press, Canada, 62-67.

17. Ganeless J, Listgarten MA, Evian CI (1986). Ultrastructure of apatite - periodontal tissue interface in human intrabony defects. *J. Periodontol.* **57**, 133-140.

18. Gourlay GJ, Rice RM, Hegyelli AF, Wade CWR, Dillon JG, Jaffe H, Kulkarni RK (1978). Biocompatibility testing of polymers: *In vivo* implantation studies. *J. Biomed. Mater. Res.* **12**, 219-232.

19. Groot K de (1981). Ceramics of calcium phosphates: preparation and properties. in: *Bio-ceramics of Calcium Phosphate*. CRC Press, Boca Raton, Florida, 99-114.

20. Hench LL, Splinter RJ, Allen WC, Greenlee TK (1972). Bonding mechanism at the interface of ceramic prosthetic materials. *J. Biomed. Mater. Res. Symp.* **4**, 117-141.

21. Jarcho M (1981). Calcium phosphate ceramics as hard tissue prosthetics. *Clin. Orthop. Rel. Res.* **157**, 259-278.

22. Kokubo T (1991). Recent progress in glass based materials for biomedical applications. *J. Ceramic Society Japan* **99**, 965-973.

23. LeGeros RZ, Orly J, Gregoire M, Daculsi G (1991). Substrate surface dissolution and interfacial biological mineralization. In: *The Bone Biomaterial Interface*. University of Toronto Press, Canada, 76-88.

24. Neo M, Kotani S, Fujita Y, Nakamura T, Yamamuro T (1991). Differences in ceramic-bone interface between surface active ceramics and resorbable ceramics: A study by scanning and transmission electron microscopy. *J. Biomed. Mater. Res.* **26**, 255-267.

25. Osborn JF, Newesly H (1980). Dynamic aspects of the implants bone interface. In: *Dental Implants*. Carl Hansen Verlag Munich, Germany, 111-123.

26. Poldrugo F, Barker S, Basa M, Massardi F, Snead OC (1985). Ethanol potentiates the toxic effects of 1.4 butanediol alcoholism. *Clin. and Exp. Res.* **9**, 493-497.

27. Sautier JM, Nefussi JR, Forest N (1991). Ultrastructural study of bone formation on synthetic hydroxyapatite in osteoblast cultures. *Cells and Materials* **1**, 209-217.

28. Schakenraad JM, Dijkstra PJ (1991). Biocompatibility of poly (DL-lactic acid glycine) copolymers. *Clinical Materials* **7**, 253-269.

29. Scherft JP (1972). The lamina limitans of the organic matrix of calcified cartilage and bone. *J. Ultrastruct. Res.* **38**, 318-331.

30. Smyth HE, Carpenter CP, Weil CS (1955). The chronic oral toxicity of the polyethylene glycols. *J. Am. Pharm. Ass.* **44**, 27-30.

31. Soballe K, Brockstedt-Rasmussen, Stender Hansen E, Büniger C (1992). Hydroxyapatite coatings modifies implant membrane formation. *Acta Orthop Scand* **63**, 128-140.

32. Thoma RJ, Hung TQ, Nyilas E, Haubold AO, Phillips RE (1987). Metal ion complexation of poly(ester) urethanes. In: *Advances in Biomedical Polymers*. Plenum Press, New York, 131-145.

33. Tracy BM, Doremus RH (1984). Direct electron microscopy studies of the bone hydroxyapatite interface. *J. Biomed. Mater. Res.* **18**, 719-726.

34. Yamamuro T, Tagai H (1991). Bone bonding behaviour of biomaterials with different surface characteristics under load bearing conditions. In: *The Bone Biomaterial Interface*. University of Toronto Press, 406-414.

35. Wagener KB (1982). Biocompatible Copolymers. US Patent number 4.350.806.

## Discussion with Reviewers

**J.M. Sautier:** Different bonding zones are shown at the transmission electron microscopy (TEM) level. Do you think that there is a relationship between the bone-bonding quality and the morphology of the interface? Have you, for example, estimated the bone-bonding by pull-out tests?

**Authors:** We indeed feel that there is a relation between the bone-bonding quality and the morphology of the interface. Especially in some more recent (unpublished) studies we were well able to demonstrate that more bone-ingrowth and interfacial contact would be obtained when using PEO/PBT copolymers that showed high rates of calcification. Since such polymers also showed a more prominent structure at the interface with bone, one would tend to think that there is a relation between interfacial morphology and quality of bonding. Also some recent studies on several calcium phosphate ceramics were indicative for a delayed appearance of the electron dense structure with slowly degrading coatings, like fluoroapatite, indicating that a relation with the activity of the ceramic is indeed present. Concerning the use of pull-out studies, although this seems to be interesting it is actually quite complicated due to the fact that with different PEO/PBT proportions the materials will also have different mechanical properties which would make a correct interpretation of pull-out data very complicated, if possible at all.

**J.M. Sautier:** Calcium absorption by the PEO segment seems to play a role in the calcification of the polymer, however the mechanism of Ca-P formation is not clear. *In vitro* studies could provide, in the future, more information on this process, particularly if the presence of cell is necessary for polymer calcification.

**Authors:** We agree with you. Such studies are currently in progress.

**J.M. Sautier:** When looking at the different morphology of the bone-bonding zone at the TEM level, do you think there is a relationship between the degradation rate of the polymers and the structure of the electron-dense layer? In this connection, do you think that degradation of the implant and products released into tissues will have a biological effect?

**Authors:** We believe that there exists a relation between calcification and the appearance of the interfacial structure. Since the polymers that show most calcification do also degrade the fastest, there is indeed a relation, although presumably indirect, between degradation and the occurrence of the electron dense layer.

It might potentially be so that a release of terephthalate from the polymer during degradation would, due to a low solubility product, lead to a calcium terephthalate precipitation which might then trigger a further calcium phosphate precipitation. Such a

precipitate might then affect the interfacial cellular phenotype. With the exception of the release of terephthalate during degradation, which has been demonstrated, this assumption is up to now purely hypothetical.

**J.M. Sautier:** Since calcification of the copolymer occurs in non-osseous sites, do you think that these materials can be qualified as "osteoinductive"?

**Authors:** So far we do not have any indications for an osteoinductive nature of these polymers. Their activity seems to be confined to osteoconductivity.

**J.M. Sautier:** You clearly demonstrated that PEO/PBT influenced the degradation rate of the copolymer. Do you think that these biomaterials could be also used for clinical application as delivery systems?

**Authors:** We are currently investigating the potential of this class of polymers as a drug delivery device. The first pilot studies indicate that, through some adaptations, these polymers might indeed be a valuable asset to the already available drug delivery polymers.

**T. Kitsugi:** In discussing Figure 12, you state "Higher magnifications demonstrated that such spots were composed of needle-like crystals"; this statement is subjective since there is no evidence. It is very difficult to define crystals and state their nature from the morphological observations alone, it is necessary to use the X-ray diffraction to characterize a crystal!

**Authors:** To see that the crystals are present (and to recognize their shape), poses no problem with the techniques we currently use; determining their nature is another matter. This is currently the subject of a different study where we are using X-ray diffraction, infrared spectroscopy, and high resolution TEM to investigate the crystal structures.

**T. Kitsugi:** It is difficult to conclude degradation from the observation of the crack since there is a possibility that the crack may have occurred during the process of making the samples.

**Authors:** Although this might indeed be a preparation artefact, it should be realized that it was only found for this specific PEO/PBT proportion after a specific post-operative interval. In other words, it is indicative for specific material changes.

**T. Kitsugi:** In Figure 14, it is very hard to distinguish the difference between the various micrographs showing the electron dense structures at the interfaces of these PEO/PBT copolymers. Could you please elaborate on that.

**Authors:** As explained in **Results**, there seems to be a clear trend relating to these electron dense interfacial structures. Whereas, the structure is very prominent with a soft material, such as PEO/PBT 70/30, in which case, it even clearly penetrates the implant surface; it gradually becomes less prominent

(thinner) when the implant contains more hard segment. Furthermore, with the PEO/PBT 55/45 we see the appearance of another more electron dense and floccular material at the interface together with the structure showing fine granular morphology that characterized the softer materials. With the PEO/PBT 40/60 this floccular material is the only characteristic interfacial structure in the absence of the finer precipitate.

The micrograph of the PEO/PBT 30/70 (Fig. 14a) deserves a special explanation. First of all this is from a sample after the 6 month evaluation period in contrast to the 6 weeks for the other PEO/PBT proportions shown in Figures 14b to 14e. This was so because, before this period, no interfacial contact was observed between the bone and the implant. Although at first sight, the structure seems rather similar to that seen for the PEO/PBT 60/40, it should be noted that it is composed of very distinct lamellar structures in comparison to the more granular appearance of the other structure. In addition, we never found a bone - PEO/PBT 30/70 contact with non-decalcified sections which indicates that this structure is most likely non-calcified.

**T. Kitsugi:** Glass-ceramics containing apatite and wollastonite is now used as an artificial bone in vertebral body. ... Dr. Kokubo (Kyoto University) published a new coating method of apatite to polymer [Kokubo T (1992). Bioactivity of glasses and glass ceramics. In: Bone-Bonding Biomaterials. Reed Healthcare Publications, Leiderdorp, Netherlands, 31-46]

**Authors:** Thank you for your comment.